

Uncertainty-Aware Dual-Ranking Strategy for Offline Data-Driven Multi-Objective Optimization

Huanbo Lyu¹, Daniel Herring², Shiqiao Zhou¹, Miqing Li¹, Zheming Zuo¹, Jelena Ninic³, James Andrews², Fabian Spill², Shuo Wang^{*1},

¹School of Computer Science, University of Birmingham, UK

²School of Mathematics, University of Birmingham, UK

³Department of Engineering, Durham University, UK

hxl099@student.bham.ac.uk, d.g.herring@bham.ac.uk, sxz363@student.bham.ac.uk, m.li.8@bham.ac.uk, z.zuo.1@bham.ac.uk, jelena.ninic@durham.ac.uk, j.w.andrews@bham.ac.uk, f.spill@bham.ac.uk, s.wang.2@bham.ac.uk

Abstract

Offline data-driven Multi-Objective Optimization Problems (MOPs) rely on limited data from simulations, experiments, or sensors. This scarcity leads to high epistemic uncertainty in surrogate predictions. Conventional surrogate methods such as Kriging assume Gaussian distributions, which can yield suboptimal results when the assumptions fail. To address these issues, we propose a simple yet novel dual-ranking strategy, working with a basic multi-objective evolutionary algorithm, NSGA-II, where the built-in non-dominated sorting is kept and the second rank is devised for uncertainty estimation. In the latter, we utilize the uncertainty estimates given by several surrogate models, including Quantile Regression (QR), Monte Carlo Dropout (MCD), and Bayesian Neural Networks (BNNs). Concretely, with this dual-ranking strategy, each solution's final rank is the average of its non-dominated sorting rank and a rank derived from the uncertainty-adjusted fitness function, thus reducing the risk of misguided optimization under data constraints. We evaluate our approach on benchmark and real-world MOPs, comparing it to state-of-the-art methods. The results show that our dual-ranking strategy significantly improves the performance of NSGA-II in offline settings, achieving competitive outcomes compared with traditional surrogate-based methods. This framework advances uncertainty-aware multi-objective evolutionary algorithms, offering a robust solution for data-limited, real-world applications.

Code — <https://anonymous.4open.science/r/26559AAAI>

Introduction

In real-world scenarios, many Multi-Objective Optimization Problems (MOPs) involve multiple conflicting objectives, with lacking analytical functions or simulation models for direct evaluation (Mazumdar et al. 2022). Consequently, data-driven Multi-Objective Evolutionary Algorithms (MOEAs) have gained prominence by combining predictive data-driven techniques with the robust search capabilities of MOEAs. These methods have proven effective in various applications, including trauma systems, airfoil design, energy systems, and smart building optimization (Jin

et al. 2018; Wang et al. 2018; Liu, Wang, and Jin 2022; Lyu et al. 2024, 2025).

Despite their success, offline data-driven MOEAs encounter a significant challenge: objective values are estimated using surrogate models (*i.e.* data-driven methods), but no new data is available to update the models or conduct real evaluations. Even with a noise-free offline dataset, the approximation uncertainty from surrogate models can largely affect optimization performance (Kim et al. 2025; Wang et al. 2018). This uncertainty may misguide the search process, resulting in suboptimal solutions. In real-world scenes *e.g.* optimizing indoor layouts in smart buildings to minimize predicted energy consumption and thermal comfort, this uncertainty can trigger suboptimal space configurations.

To mitigate this uncertainty, various ensemble learning-based methods have been proposed, such as selective surrogate ensembles (Wang et al. 2018), perturbation-based ensemble surrogates (Li et al. 2020) and ensemble surrogates with tri-training (Huang, Wang, and Jin 2021). Nevertheless, these methods do not directly incorporate uncertainty information into the optimization process. Consequently, the accumulation of prediction errors during optimization can sharply compromise the search process, potentially leading to suboptimal outcomes (Liu, Wang, and Jin 2022).

In offline data-driven MOPs, Kriging is commonly adopted as a surrogate model due to its ability to yield uncertainty estimates, including predicted means and standard deviations (Li, Li, and Azarm 2008). Several methodologies leverage this information, such as adaptive model selection (Liu, Wang, and Jin 2022), probabilistic selection mechanisms (Liu, Wang, and Jin 2022) and extensions to constrained MOPs (Zhang et al. 2024a,b). However, Kriging suffers from high computational complexity, scaling at $O(N^3)$ (Hensman, Fusi, and Lawrence 2013), and its reliance on Gaussian data distribution assumptions can impair predictive accuracy. Thus, there is a pressing need for surrogate models that can efficiently manage datasets, improve predictive performance, and provide reliable uncertainty quantification.

This work presents a novel dual-ranking strategy for offline data-driven MOEAs under uncertainty, with the following major contributions.

- **Flexible Integration with Surrogate Models.** The dual-

ranking strategy seamlessly integrates with various surrogate models that provide uncertainty quantification, such as Kriging, Quantile Regression (QR) (Koenker and Hallock 2001), Monte Carlo Dropout (MCD) (Gal and Ghahramani 2016), and Bayesian Neural Network (BNN) (Blundell et al. 2015). It incorporates predictive results and uncertainty estimates into an adjusted fitness function to enhance optimization robustness.

- **Enhanced Survival Selection in NSGA-II.** The dual-ranking strategy is applied during the survival selection phase of Non-dominated Sorting Genetic Algorithm II (NSGA-II). It performs non-dominated sorting on both the original and adjusted fitness functions, computing each solution’s rank by averaging its ranks across the two sorts for each non-dominated front, thereby improving solution diversity and quality.
- **Comprehensive Evaluation.** The approach is rigorously evaluated against state-of-the-art methods on 14 synthetic and real-world benchmark problems, demonstrating superior performance and effectiveness in handling uncertainty in multi-objective optimization.

Preliminaries

Multi-Objective Optimization

We consider the MOPs of the following form:

$$\begin{aligned} & \text{minimize } \mathbf{f}(\mathbf{x}) = (f_1(\mathbf{x}), f_2(\mathbf{x}), \dots, f_K(\mathbf{x})) \\ & \text{subject to } \mathbf{x} \in S \end{aligned} \quad (1)$$

where \mathbf{x} is the decision vector, $K \geq 2$ is the total number of objectives, and S is the feasible region in the decision space. A solution $\mathbf{x}_1 \in S$ dominates another solution $\mathbf{x}_2 \in S$, indicated as $\mathbf{x}_1 \prec \mathbf{x}_2$, if $f_k(\mathbf{x}_1) \leq f_k(\mathbf{x}_2)$ for all $k = 1, \dots, K$ and $f_k(\mathbf{x}_1) < f_k(\mathbf{x}_2)$ for at least one $k = 1, \dots, K$. The set of solutions that cannot be dominated by any other feasible solution is the Pareto Set (PS), and the set of their objective values is the Pareto Front (PF).

Offline Data-Driven Multi-Objective Optimization

In offline data-driven MOPs, there is no explicit mathematical expression for the objective function, nor is it possible to acquire or evaluate new data points from real-world experiments or physical simulations during the optimization process (Liu, Wang, and Jin 2022; Mazumdar et al. 2022). Only a pre-collected dataset is available, and this offline dataset remains fixed during optimization. The objective functions are approximated by training surrogate models on this offline dataset.

Uncertainty In offline data-driven MOPs, uncertainty may arise from the estimation errors. This uncertainty, introduced by surrogate models, can misguide the search process, resulting in the selection of solutions with worse underlying objective values. For example, in Figure 1, we consider a minimization problem with two objectives f_1, f_2 , and two underlying solutions, \mathbf{A} (blue) and \mathbf{B} (red), shown in the objective space. Based on the surrogate evaluations, $f_{\text{sur}}(\mathbf{A})$ is better than $f_{\text{sur}}(\mathbf{B})$ in both objectives, implying $\mathbf{A} \prec \mathbf{B}$. However, the real value $f_{\text{real}}(\mathbf{A})$ (triangle) is worse

than $f_{\text{real}}(\mathbf{B})$ in both objectives, meaning that $\mathbf{B} \prec \mathbf{A}$. This example shows that relying solely on surrogate evaluations can lead to incorrect selection during optimization. Therefore, uncertainty information should be incorporated into the optimization algorithm to mitigate such issues.

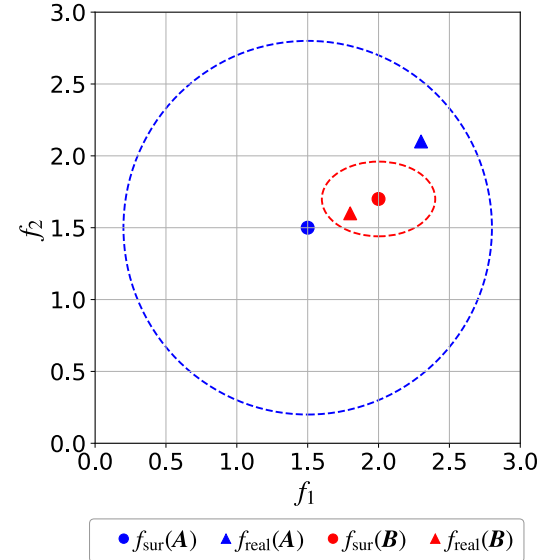


Figure 1: Example of solution ranking in a multi-objective minimization problem, showing how surrogate evaluations ($f_{\text{sur}}(\mathbf{A}), f_{\text{sur}}(\mathbf{B})$) may misjudge the Pareto dominance relation due to prediction uncertainty, with the dashed circle denoting the uncertainty interval.

Surrogate Modeling

In data-driven MOPs, the surrogate model \mathcal{M} aims to predict the objective values of a potential solution \mathbf{x} , and is trained on the given offline dataset \mathcal{D} where no new data can be acquired. For each objective, a surrogate model is trained, resulting in a total of K surrogate models. For a given solution \mathbf{x} , the k -th objective value $f_k(\mathbf{x})$ estimated from the surrogate model \mathcal{M}_k can be represented as:

$$f_k(\mathbf{x}) \approx \mathcal{M}_k(\mathbf{x}). \quad (2)$$

Our work will be evaluated using surrogate models trained by following machine learning methods.

Kriging The Kriging model (Li, Li, and Azarm 2008; Liu, Wang, and Jin 2022) estimates the output at a new sample \mathbf{x} as:

$$\hat{y} = \mu(\mathbf{x}) + \epsilon(\mathbf{x}), \quad (3)$$

where \hat{y} is the predicted objective value, $\mu(\mathbf{x})$ represents the global trend of the data, and $\epsilon(\mathbf{x})$ is a zero-mean Gaussian process, *i.e.* $\epsilon(\mathbf{x}) \sim \mathcal{GP}(0, k(\mathbf{x}, \mathbf{x}'))$. We incorporate $\mu(\mathbf{x})$ and $\epsilon(\mathbf{x})$ into the surrogate model to leverage uncertainty information.

Quantile Regression The Ordinary Least Squares (OLS) regression (Greene 2003) estimate the conditional mean of y_i by minimizing the sum of squared residuals:

$$\hat{\beta} = \arg \min_{\beta} \sum_{i=1}^n (y_i - \mathbf{x}_i^\top \beta)^2, \quad (4)$$

where, \mathbf{x}_i is the vector of independent variables, β represents the regression coefficients. The conditional quantile (e.g. median) of the target variable (Koenker and Hallock 2001) is estimated by QR. For a given quantile level $\tau \in (0, 1)$, the function is:

$$\hat{\beta}_\tau = \arg \min_{\beta} \sum_{i=1}^n \rho_\tau(y_i - \mathbf{x}_i^\top \beta), \quad (5)$$

where the loss function $\rho_\tau(u)$ is the “check function” (Steinwart and Christmann 2011), defined as

$$\rho_\tau(u) = \begin{cases} \tau u, & \text{if } u \geq 0 \\ (1-\tau)u, & \text{if } u < 0, \end{cases} \quad (6)$$

The simplicity and generality of this formulation makes quantile regression widely applicable across various domains (Romano, Patterson, and Candes 2019). We employ QR to obtain estimated uncertainty intervals by leveraging the predictive outputs at different quantile levels.

Monte Carlo Dropout MCD is an approximate Bayesian inference technique that enables uncertainty estimation in neural networks by interpreting dropout as a variational approximation to a deep Gaussian process (Gal and Ghahramani 2016). To estimate the predictive distribution at a new input \mathbf{x} , the model is evaluated T times with dropout activated, yielding a set of stochastic outputs $\{\hat{y}_t\}_{t=1}^T$. The predictive output can then be represented as:

$$E[y] \approx \frac{1}{T} \sum_{t=1}^T \hat{y}_t, \quad (7)$$

$$\text{Var}(y) \approx \frac{1}{T} \sum_{t=1}^T \hat{y}_t^2 - \left(\frac{1}{T} \sum_{t=1}^T \hat{y}_t \right)^2, \quad (8)$$

where $E[y]$ denotes the predictive mean, and $\text{Var}(y)$ represents the predictive variance (i.e. epistemic uncertainty). We use $E[y]$ and $\text{Var}(y)$ to represent predictive uncertainty information in surrogate models.

Bayesian Neural Network BNN places probability distributions over the network weights instead of point estimates, enabling the modeling of epistemic uncertainty (Blundell et al. 2015). Given a training dataset \mathcal{D} , BNN aims to approximate the posterior distribution $p(\mathbf{w} | \mathcal{D})$ over weights \mathbf{w} using variational inference. For a given input \mathbf{x} , the predictive distribution is approximated as:

$$p(y | \mathbf{x}) \approx \frac{1}{S} \sum_{s=1}^S p(y | \mathbf{x}, \mathbf{w}^{(s)}), \quad \mathbf{w}^{(s)} \sim q(\mathbf{w}), \quad (9)$$

where $q(\mathbf{w})$ is the learned variational posterior.

Uncertainty-Aware Dual-Ranking Strategy

In offline data-driven MOPs, leveraging uncertainty information during optimization is crucial to avoid misguiding search that incorrect judgments of dominance relationships between solutions caused by inaccurate surrogate predictions. Existing methods often rely on the predictive mean and standard deviation from Kriging models to adjust model selection or perform Monte Carlo sampling. However, these methods are typically limited to Kriging, relies on Gaussian assumptions that may not hold for all data and may suffer from high computational cost. In this work, we consider a different perspective that directly incorporates uncertainty information into the ranking process of NSGA-II. We propose the dual-ranking strategy that utilizes both the original and uncertainty-adjusted fitness functions. Our method can be flexibly integrated with various surrogate models that provide uncertainty estimates. An overview of the proposed method is shown in Figure 2, and the detailed procedure is described in the following sections.

Adjusted Fitness Functions

In offline data-driven MOPs, leveraging uncertainty information is essential to avoid incorrect dominance judgments caused by inaccurate surrogate predictions. We adopt surrogate models including Kriging, QR, MCD and BNN to output the predictive results with uncertainty estimates. For a candidate solution \mathbf{x} , the k -th objective value $f_k(\mathbf{x})$ is approximated by surrogate models that provide both predictive results and uncertainty estimates. For QR, we select two quantile (e.g. median at $\tau = 0.5$ and upper at $\tau = 0.9$), and the objective values are denoted as $f_k^{\text{QR}}(\mathbf{x})$. For other surrogate models including Kriging, MCD and BNN, we simplify the representation as (μ_k, σ_k) to indicate the predictive results and uncertainty estimates. The objective values are denoted as $f_k^{\text{other}}(\mathbf{x})$. Based on the Equation 2, we have:

$$f_k^{\text{QR}}(\mathbf{x}) \approx \mathcal{M}_k^{\text{QR}}(\mathbf{x}) = (q_k^{\text{median}}(\mathbf{x}), q_k^{\text{upper}}(\mathbf{x})), \quad (10)$$

$$f_k^{\text{other}}(\mathbf{x}) \approx \mathcal{M}_k^{\text{other}}(\mathbf{x}) = (\mu_k(\mathbf{x}), \sigma_k(\mathbf{x})). \quad (11)$$

During optimization, the surrogate prediction for each solution is used to compute two types of fitness values: an original fitness value and an adjusted one that incorporates uncertainty. The original fitness function $f_{k,\text{ori}}(\mathbf{x})$ is defined as:

$$f_{k,\text{ori}}^{\text{QR}}(\mathbf{x}) = q_k^{\text{median}}(\mathbf{x}), \quad (12)$$

$$f_{k,\text{ori}}^{\text{other}}(\mathbf{x}) = \mu_k(\mathbf{x}). \quad (13)$$

To reduce the risk of incorrect dominance relationships caused by high-uncertainty predictions, we incorporate uncertainty directly into fitness evaluation. Inspired by the Gaussian Process Upper Confidence Bound (GP-UCB) principle (Srinivas et al. 2009), we define an adjusted fitness function $f_{k,\text{adj}}(\mathbf{x})$ that penalizes solutions with large predictive uncertainty:

$$f_{k,\text{adj}}^{\text{QR}}(\mathbf{x}) = q_k^{\text{upper}}(\mathbf{x}), \quad (14)$$

$$f_{k,\text{adj}}^{\text{other}}(\mathbf{x}) = \mu_k(\mathbf{x}) + z \cdot \sigma_k(\mathbf{x}). \quad (15)$$

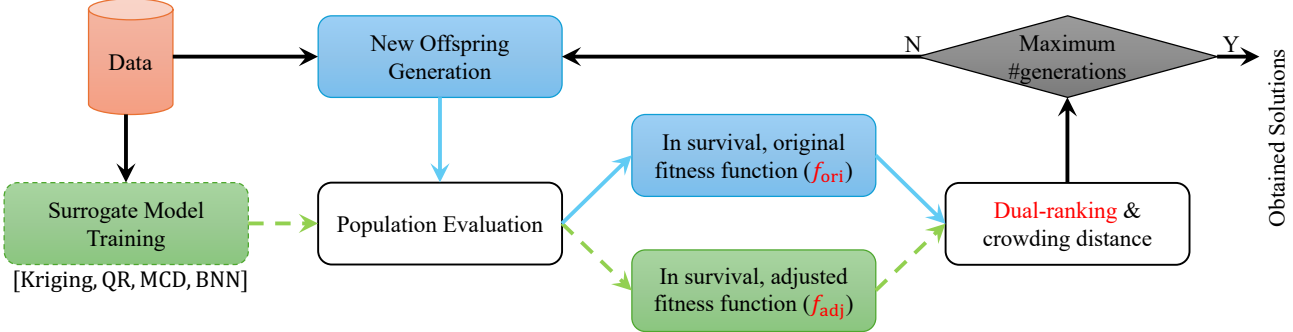


Figure 2: Workflow of the enhanced non-dominated-sorting-based MOEA, in which the improvement is contributed by our proposed Dual-Ranking (DR) strategy. DR is the integration of rankings coming from the surrogate model training and conventional optimization process.

Larger uncertainty estimates from the surrogate models may give more inaccurate evaluations which increases the probability of incorrectly changing the dominance relationship between solutions. Therefore, the *adjusted* fitness function penalizes large uncertainty estimates in minimizing problems. For $f_{k,\text{adj}}^{\text{QR}}(\mathbf{x})$, the upper quantile q_k^{upper} captures predictive uncertainty, and its value is determined by the selected quantile level τ (e.g. $\tau = 0.9$). For $f_{k,\text{adj}}^{\text{other}}(\mathbf{x})$, the coefficient $z = \Phi^{-1}(\tau)$ (Casella and Berger 2024) is the inverse cumulative distribution function (CDF) of the standard normal distribution evaluated at quantile level τ , e.g. $z \approx 1.28$ when $\tau = 0.9$.

Dual-Ranking Strategy

In the survival phase of optimization algorithms, each candidate solution is evaluated using both the original $f_{\text{ori}}(\mathbf{x})$ and the uncertainty-adjusted $f_{\text{adj}}(\mathbf{x})$ fitness functions, as defined in the previous section. The dual-ranking strategy aims to balance exploitation (favoring low predictive objectives) and robustness (using high uncertainty). Specifically, standard non-dominated sorting are performed separately on the population evaluated by the original $f_{\text{ori}}(\mathbf{x})$ and adjusted $f_{\text{adj}}(\mathbf{x})$ fitness function. From these two non-dominated fronts, each solution is assigned two ranks: one based on the original fitness value and one based on the uncertainty-adjusted value. The final rank of each solution is computed as the average of these two ranks. This method prioritizes solutions that are both high-quality and reliable, while still retaining those that exhibit either high-quality with relatively higher uncertainty or low uncertainty with slightly worse objectives. After obtaining the final ranks, non-dominated fronts are reconstructed accordingly. In the subsequent crowding distance calculation, only the original fitness values are used, keeping consistency with the standard NSGA-II procedure.

The pseudo-code is presented in Algorithms 1 and 2. The inputs consist of the population P_{ori} evaluated by the original fitness function $f_{\text{ori}}(\mathbf{x})$, and the population P_{adj} evaluated by the adjusted fitness function $f_{\text{adj}}(\mathbf{x})$. The population size is N . After applying non-dominated sorting separately to P_{ori} and P_{adj} , the final rank r_{avg} is obtained by averaging the ranks r_{ori} and r_{adj} , which are derived from the corresponding

non-dominated fronts \mathcal{F}_{ori} and \mathcal{F}_{adj} , respectively. The output is the hybrid non-dominated front \mathcal{F}_{hyb} , constructed using the average rank.

Algorithm 1: ComputeRank(P)

```

1: Input: population  $P$ .
2: Output: Rank  $r$  .
3:  $\mathcal{F} \leftarrow \text{NonDominatedSorting}(P)$ 
4: for  $i \leftarrow 0$  to  $N$  do
5:    $r[i] \leftarrow -1$ 
6: end for
7: for  $i \leftarrow 0$  to  $\text{length}(\mathcal{F}) - 1$  do
8:   for  $p \in \mathcal{F}[i]$  do
9:      $r[p] \leftarrow i$ 
10:  end for
11: end for

```

We analyze the time complexity of the proposed dual-ranking strategy. The standard non-dominated sorting procedure in NSGA-II has a time complexity of $O(MN^2)$, where N is the number of candidate solutions and M is the number of objectives. The dual-ranking strategy performs two such sorting operations $2 \cdot O(MN^2) = O(MN^2)$. The additional operations, including constructing ranking arrays, computing average ranks, and rebuilding the hybrid fronts, require only $O(N)$ time. In summary, the overall time complexity of the dual-ranking strategy remains $O(MN^2)$.

Experiments

Experimental Setup

Benchmark Problems We consider 14 synthetic and real-world benchmark problems for comparative experiments, including DTLZ 1-7 (Deb et al. 2005) with 2 objectives and 10 decision variables, Kursawe (Kursawe 1990), Truss2D (Deb and Srinivasan 2006), Welded Beam (Deb and Kalyanmoy 2001), BNH (Binh and Korn 1997), MODAct CS 1-3 (Picard and Schiffmann 2020). It is worth noting that Truss2D, Welded Beam, BNH, and MODAct CS 1-3 are constrained MOPs.

Method	DTLZ1	DTLZ2	DTLZ3	DTLZ4	DTLZ5	DTLZ6	DTLZ7	Kursawe	Truss2D	Welded Beam	BNH	CS1	CS2	CS3
Kriging	1.11e+4	2.28e-2	6.71e+4	3.07e-2	2.28e-2	2.42e-2	1.12e-1	2.01e+1	8.03e+9	4.30e+2	2.00e-2	7.36e+3	7.36e+3	7.36e+3
QR	5.18e+3	3.61e-2	2.80e+4	2.03e-2	3.61e-2	6.46e-2	9.82e-2	7.67	3.40e+9	6.37e+2	5.34e+1	6.57e+3	6.57e+3	6.57e+3
MCD	4.79e+3	3.96e-2	2.75e+4	3.58e-2	3.99e-2	4.59e-2	9.91e-2	7.91	6.50e+9	1.78e+3	2.63	8.39e+3	8.51e+3	8.37e+3
BNN	6.20e+3	4.29e-2	4.15e+4	7.39e-2	4.15e-2	2.83e-2	4.00e-2	8.22	2.96e+9	4.62e+3	1.99	8.14e+3	7.55e+3	7.60e+3

Table 1: The predictive performance of all surrogate models is evaluated across 14 benchmark problems using Mean Squared Error (MSE). The lowest MSE for each problem is marked in **bold**. Unconstrained and constrained problems are denoted with normal and *italic*.

Method	DTLZ1		DTLZ2		DTLZ3		DTLZ4		DTLZ5	
	MSE (e+4)	HV (e+5)	MSE (e-2)	HV	MSE (e+5)	HV (e+6)	MSE	HV	MSE (e-2)	HV
Kriging+DR	3.72 ± 0.90	6.01 ± 0.15	4.61 ± 0.20	8.19 ± 0.00	1.81 ± 0.44	2.06 ± 0.08	2.28 ± 0.18	6.69 ± 0.15	4.61 ± 0.20	8.19 ± 0.00
QR+DR	0.42 ± 0.19	6.06 ± 0.13	4.15 ± 1.05	7.87 ± 0.06	0.32 ± 0.13	1.99 ± 0.09	0.05 ± 0.01	5.89 ± 0.06	4.15 ± 1.05	7.87 ± 0.06
MCD+DR	0.55 ± 0.44	5.69 ± 0.25	6.91 ± 2.98	7.24 ± 0.16	0.42 ± 0.20	1.84 ± 0.10	0.21 ± 0.10	5.59 ± 0.15	7.28 ± 2.42	7.20 ± 0.17
BNN+DR	2.26 ± 0.27	6.24 ± 0.06	11.40 ± 4.56	6.78 ± 0.24	0.60 ± 0.17	2.16 ± 0.03	0.13 ± 0.04	4.59 ± 0.33	18.58 ± 4.11	6.57 ± 0.20
Prob-RVEA	2.20 ± 1.12	5.74 ± 0.16	3.38 ± 0.23	8.10 ± 0.01	2.42 ± 0.69	1.93 ± 0.09	0.72 ± 0.16	7.08 ± 0.26	3.27 ± 0.24	8.09 ± 0.01
Prob-MOEA/D	0.87 ± 0.29	5.68 ± 0.14	1.87 ± 0.37	7.98 ± 0.03	0.76 ± 0.55	1.84 ± 0.14	0.36 ± 0.18	6.72 ± 0.42	2.27 ± 0.36	8.00 ± 0.02
IBEA-MS	1.08 ± 0.83	6.12 ± 0.16	6.56 ± 0.71	8.14 ± 0.03	0.82 ± 0.52	2.16 ± 0.07	0.02 ± 0.00	6.30 ± 0.44	6.49 ± 0.81	8.14 ± 0.05
Method	DTLZ6		DTLZ7		Kursawe		Truss2D		Welded Beam	
	MSE (e-1)	HV (e+1)	MSE	HV (e+1)	MSE (e+1)	HV (e+2)	MSE (e+9)	HV (e+3)	MSE (e+2)	HV
Kriging+DR	1.91 ± 0.70	5.96 ± 0.14	1.13 ± 0.34	2.77 ± 0.05	1.60 ± 0.27	0.96 ± 0.05	0.54 ± 0.25	7.33 ± 0.43	1.99 ± 0.16	2.71 ± 0.52
QR+DR	0.99 ± 0.26	4.63 ± 0.16	7.74 ± 0.38	3.42 ± 0.01	1.25 ± 0.21	1.11 ± 0.10	0.40 ± 0.13	6.79 ± 0.01	1.24 ± 0.17	2.96 ± 0.06
MCD+DR	1.93 ± 0.67	5.39 ± 0.20	0.12 ± 0.01	3.26 ± 0.07	3.18 ± 0.62	0.89 ± 0.09	1.39 ± 0.21	7.43 ± 0.30	3.76 ± 0.11	2.39 ± 0.11
BNN+DR	0.97 ± 0.40	5.63 ± 0.19	0.21 ± 0.04	3.38 ± 0.01	1.31 ± 0.17	1.17 ± 0.04	1.49 ± 0.58	6.02 ± 0.78	3.68 ± 0.15	2.75 ± 0.06
Prob-RVEA	0.22 ± 0.04	3.56 ± 0.15	0.36 ± 0.04	2.68 ± 0.04	1.84 ± 0.47	1.03 ± 0.05	-	-	-	-
Prob-MOEA/D	0.08 ± 0.02	3.16 ± 0.10	0.40 ± 0.12	2.95 ± 0.03	0.96 ± 0.23	0.96 ± 0.05	-	-	-	-
IBEA-MS	37.11 ± 18.42	8.89 ± 0.72	0.06 ± 0.02	3.44 ± 0.03	2.64 ± 3.83	1.25 ± 0.26	-	-	-	-
Method	BNH		CS1		CS2		CS3			
	MSE (e-2)	HV (e+3)	MSE (e+4)	HV (e+1)	MSE (e+3)	HV (e+1)	MSE (e+2)	HV		
Kriging+DR	5.32 ± 0.56	5.25 ± 0.00	1.43 ± 0.60	1.69 ± 0.81	9.69 ± 5.96	3.34 ± 1.39	8.95 ± 14.25	3.40 ± 2.61		
QR+DR	5775.28 ± 457.08	5.13 ± 0.01	1.34 ± 0.51	1.31 ± 1.31	11.79 ± 5.03	6.63 ± 2.91	6.58 ± 15.37	4.13 ± 3.35		
MCD+DR	572.08 ± 66.42	5.13 ± 0.02	0.22 ± 0.09	2.17 ± 0.60	1.41 ± 0.76	5.73 ± 1.69	15.18 ± 7.25	3.55 ± 2.76		
BNN+DR	162.88 ± 24.35	5.23 ± 0.00	0.31 ± 0.10	3.51 ± 0.59	1.85 ± 0.65	5.77 ± 1.20	15.08 ± 5.99	3.74 ± 2.76		
Prob-RVEA	-	-	-	-	-	-	-	-		
Prob-MOEA/D	-	-	-	-	-	-	-	-		
IBEA-MS	-	-	-	-	-	-	-	-		

Table 2: Optimization performance on 14 benchmark problems using methods including surrogate models with Dual-Ranking (DR) (ours), Prob-RVEA, Prob-MOEA/D, and IBEA-MS, evaluated by MSE and HV. Here, MSE measures the difference between the real evaluations and the surrogate-based evaluations. For each problem, the results are reported as the mean ± standard deviation over 30 repeats. The lowest MSE and the highest HV are denoted in bold. A dash (‘-’) indicates that the corresponding algorithms cannot handle the *constrained* MOPs. The lowest MSE and highest HV for each problem are marked in **bold**. Unconstrained and *constrained* problems are denoted with normal and *italic*.

Algorithm 2: Dual-Ranking

```

1: Input: population  $P_{\text{ori}}$  evaluated by the original fitness
   function, population  $P_{\text{adj}}$  evaluated by the adjusted fitness
   function, population size  $N$ .
2: Output: non-dominated front  $\mathcal{F}_{\text{hyb}}$ .
3:  $r_{\text{ori}} \leftarrow \text{ComputeRank}(P_{\text{ori}})$ 
4:  $r_{\text{adj}} \leftarrow \text{ComputeRank}(P_{\text{adj}})$ 
5:  $r_{\text{avg}} \leftarrow \text{mean}(r_{\text{ori}}, r_{\text{adj}}) // \text{element-wise mean}$ 
6: for  $i \leftarrow 0$  to  $N$  do
7:    $\mathcal{F}_{\text{hyb}}[r_{\text{avg}}[i]] \leftarrow i$ 
8: end for
9: Remove empty sets from  $\mathcal{F}_{\text{hyb}}$ 
10: return  $\mathcal{F}_{\text{hyb}}$ 

```

Baseline Methods We compare our methods against state-of-the-art methods, including Probabilistic RVEA (Prob-RVEA), Probabilistic MOEA/D (Prob-MOEA/D) (Mazumdar et al. 2022), and IBEA implemented in Matlab (Liu, Wang, and Jin 2022). The experiments are performed over 30 independent runs, with fixed random seeds ranging from 1 to 30 unless otherwise specified.

Offline Dataset The offline data are generated using Latin Hypercube Sampling (LHS) (Helton and Davis 2003), and the random seed is fixed to 42 to ensure reproducibility. Following the default setting in (Liu, Wang, and Jin 2022), the number of samples is set to $11D - 1$ (default settings), where D denotes the number of decision variables.

Surrogate Models Kriging is implemented using the Scikit-learn python library (Pedregosa et al. 2011), with a Gaussian and constant kernel. The spread rate hyperparameter α is set to 10^{-3} to prevent overfitting. QR is implemented using AutoGluon-Tabular (Erickson et al. 2020), with quantile levels of 0.5 and 0.9, and a fixed random seed

of 42. MCD and BNN are implemented by PyTorch (Paszke et al. 2019) and Pyro (Bingham et al. 2019) respectively. Both models use a hidden dimension of 32, an initial learning rate of 10^{-3} (unless otherwise specified), the Adam optimizer (Kingma and Ba 2014). The number of training epochs is tuned for each benchmark problem. MCD uses a dropout rate of 0.1. BNN employs the AutoDiagonalNormal for variational inference. Other settings are reported in the Supplementary Material.

Optimization Algorithms The optimization framework is implemented using pymoo version 0.6.1.3 (Blank and Deb 2020). The fitness functions are revised by different surrogate models with a modified ranking process, enabling the algorithm to incorporate uncertainty information. The population size is set to 100, and the maximum number of generation is 100, resulting in a total of 10,000 fitness evaluations. For the reproduction operators, Simulated Binary Crossover (SBX) (Deb, Agrawal et al. 1995) is applied with a crossover probability of 1.0 and a distribution factor of $\eta = 20$. Polynomial mutation (Deb et al. 2002) is employed with a mutation probability of $1/D$ and the same distribution factor.

Performance Metrics The predictive performance of the surrogate models is evaluated using the classical metric MSE.

The optimization results are evaluated using the Hyper-volume (HV) (Zitzler and Thiele 1999). The reference point for the HV is chosen following the common settings for each benchmark problem, as detailed in the Supplementary Material. We report and compare only the HV values computed from real evaluations, as those based on surrogate predictions may introduce errors and potentially mislead the results (see Figure 3). For the obtained solutions, the difference between the real evaluations and the surrogate-based evaluations is measured using the MSE.

Ablation Experiments We conduct ablation experiments (see Supplementary Material) to evaluate the effects of the surrogate-based and uncertainty-adjusted fitness functions. The main findings are summarized as follows. Using only the original fitness function, Kriging and BNN perform worse, while QR and MCD are comparable or slightly worse than their dual-ranking versions on most problems. Using only the uncertainty-aware fitness function, Kriging and BNN show similar performance, whereas QR and MCD are sometimes worse and sometimes comparable to their dual-ranking versions.

Experimental Results

We first compare the predictive performance of different surrogate models across all benchmark problems. As shown in Table 1, the Kriging model, which commonly adopted by state-of-the-art methods, achieves the lowest MSE on only 5 out of 14 problems. In contrast, other surrogate models, including QR, MCD, and BNN, achieve the lowest MSE on the remaining 9 problems. In particular, Kriging performs significantly worse than the other models on DTLZ1, DTLZ3, Kursawe, and Truss2D.

We then compare the optimization performance across all benchmark problems. As shown in Table 2, our proposed methods, which combine different surrogate models with the Dual-Ranking (DR) strategy, achieve the best results in terms of both MSE and HV on DTLZ1 and DTLZ3, and obtain the highest HV on DTLZ2 and DTLZ5. In addition, our methods achieve sub-optimal but competitive performance on DTLZ4, DTLZ7, and Kursawe, demonstrating relative robustness across diverse problems. On DTLZ6, we observe that Prob-MOEAD achieves the best MSE but the worst HV, whereas IBEA-MS achieves the best HV but the worst MSE. This indicates that both methods may perform well but lacking robustness. In contrast, our DR-based methods achieve consistently good performance in both MSE and HV.

For the constrained problems, including Truss2D, Welded Beam, BNH, and MODAct CS 1–3, none of the compared state-of-the-art algorithms can handle constraints, whereas our proposed methods can solve them. Among all configurations, QR+DR demonstrates relatively competitive performance across these constrained MOPs.

Lastly, we present example Pareto fronts on the DTLZ1 benchmark problem, with the random seed fixed to 1 when applicable, using both surrogate-based and real evaluations, as shown in Figure 3. In this problem, all objective values are expected to be equal to or greater than zero. However, the results obtained from Kriging-based methods (including Kriging+DR and all state-of-the-art baselines) as well as BNN+DR, contain negative values. In contrast, solutions evaluated by the surrogate models QR and MCD yield only positive values. This suggests that surrogate-based evaluations using Kriging or BNN can introduce predictive errors that misguide the search process.

As further illustrated by the bar chart within Figure 3, Kriging-based methods (including Kriging+DR, Prob-RVEA, and IBEA-MS) and BNN+DR exhibit higher HV values under surrogate-based evaluation compared to real evaluation. This indicates potential overestimation of obtained PF. In such cases, when only surrogate-based evaluations are available, these methods may lead to unreliable decision making. In contrast, QR and MCD demonstrate more consistent behavior, making them more suitable choices for MOPs under uncertainty. Furthermore, our proposed dual-ranking strategy, which can be flexibly integrated with different surrogate models, demonstrates robustness in such situations.

Conclusion

In offline data-driven MOPs, no new data can be acquired to update the surrogate model, and the uncertainty from surrogate predictions may misguide the optimization process. Therefore, optimization methods need to handle such uncertainty during the search process. In this work, we propose the dual-ranking strategy that can be flexibly integrated with different surrogate models and directly incorporate uncertainty information into the optimization process.

The experimental results show that a Kriging surrogate model, which the state-of-the-art methods often adopted, does not achieve the best predictive performance on most

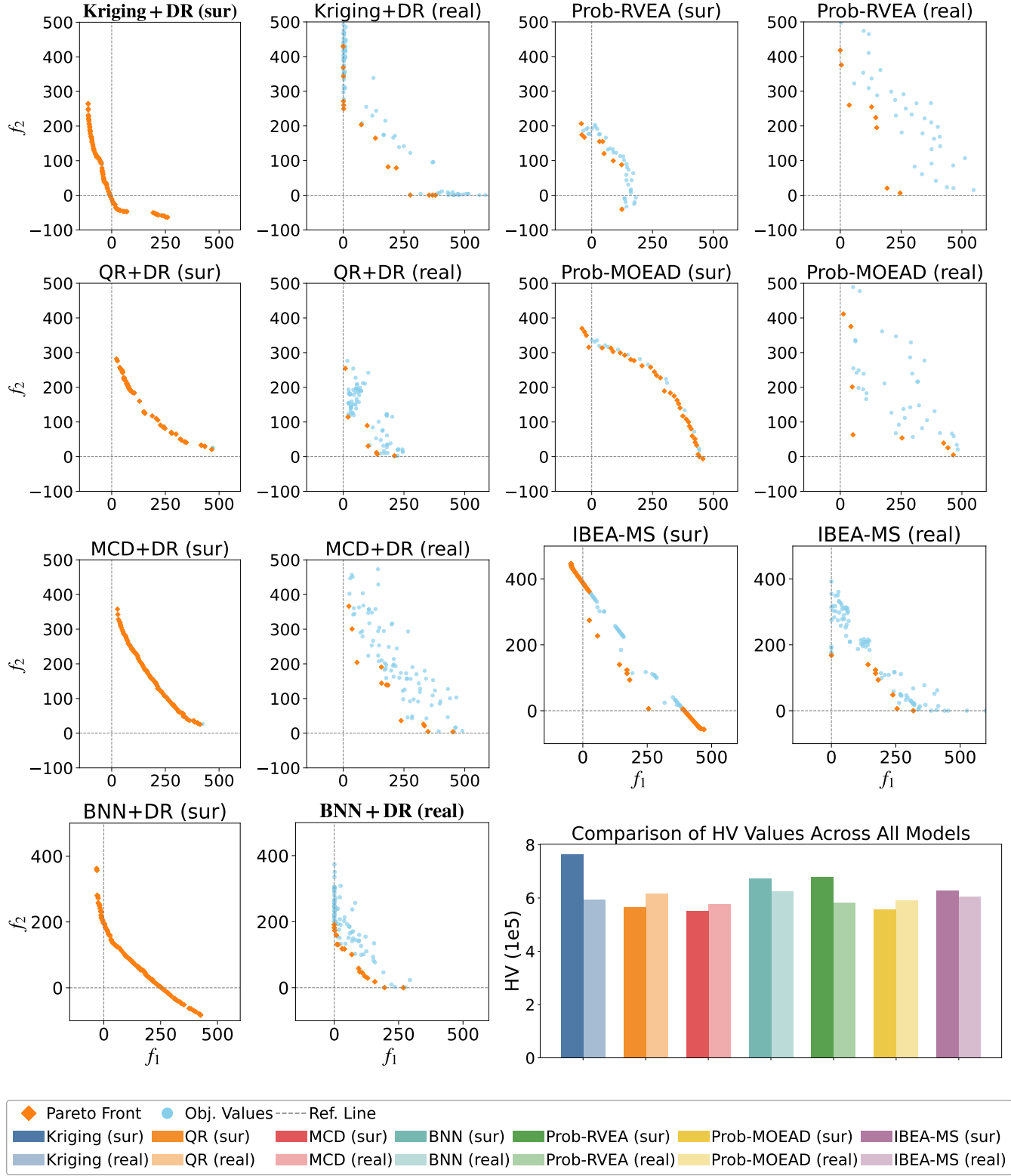


Figure 3: Pareto front obtained on DTLZ1 using surrogate-based (sur) and real (real) evaluations for all compared methods. The bar chart in the bottom-right corner summarizes the corresponding HV values, with different surrogate models indicated by different colors. The best performance based on surrogate-based and real evaluations is denoted in bold. In the legend, the first row corresponds to the plots for surrogate-based and real evaluations, while the second and third rows refer to the bar charts.

of the benchmark problems, while other surrogate models demonstrate superior performance on many problems. Our proposed dual-ranking strategy with different surrogate models, achieve the best or competitive performance on many benchmark problems. Our methods are capable of solving constrained MOPs, which the compared state-of-the-art algorithms cannot handle. As illustrated by the obtained PF on DTLZ1 (Figure 3), if optimization relies solely on surrogate-based evaluations, Kriging-based and BNN-based methods may lead to misguiding judgments of solutions, while QR and MCD provide more reliable results. Experimental results also inspire further investigation on continuously arriving data, such as data streams and online optimization scenarios.

References

Bingham, E.; Chen, J. P.; Jankowiak, M.; Obermeyer, F.; Pradhan, N.; Karaletsos, T.; Singh, R.; Szerlip, P.; Horsfall, P.; and Goodman, N. D. 2019. Pyro: Deep universal probabilistic programming. *Journal of machine learning research*, 20(28): 1–6.

Binh, T. T.; and Korn, U. 1997. MOBES: A multiobjective evolution strategy for constrained optimization problems. In *The third international conference on genetic algorithms (Mendel 97)*, volume 25, 27.

Blank, J.; and Deb, K. 2020. pymoo: Multi-Objective Optimization in Python. *IEEE Access*, 8: 89497–89509.

Blundell, C.; Cornebise, J.; Kavukcuoglu, K.; and Wierstra, D. 2015. Weight uncertainty in neural network. In *International conference on machine learning*, 1613–1622. PMLR.

Casella, G.; and Berger, R. 2024. *Statistical inference*. Chapman and Hall/CRC.

Deb, K.; Agrawal, R. B.; et al. 1995. Simulated binary crossover for continuous search space. *Complex Systems*, 9(2): 115–148.

Deb, K.; and Kalyanmoy, D. 2001. *Multi-Objective Optimization Using Evolutionary Algorithms*. USA: John Wiley & Sons, Inc. ISBN 047187339X.

Deb, K.; Pratap, A.; Agarwal, S.; and Meyarivan, T. 2002. A fast and elitist multiobjective genetic algorithm: NSGA-II. *IEEE transactions on evolutionary computation*, 6(2): 182–197.

Deb, K.; and Srinivasan, A. 2006. Innovization: Innovating design principles through optimization. In *Proceedings of the 8th annual conference on Genetic and evolutionary computation*, 1629–1636.

Deb, K.; Thiele, L.; Laumanns, M.; and Zitzler, E. 2005. Scalable test problems for evolutionary multiobjective optimization. In *Evolutionary multiobjective optimization: theoretical advances and applications*, 105–145. Springer.

Erickson, N.; Mueller, J.; Shirkov, A.; Zhang, H.; Larroy, P.; Li, M.; and Smola, A. 2020. Autogluon-tabular: Robust and accurate automl for structured data. *arXiv preprint arXiv:2003.06505*.

Gal, Y.; and Ghahramani, Z. 2016. Dropout as a bayesian approximation: Representing model uncertainty in deep learning. In *international conference on machine learning*, 1050–1059. PMLR.

Greene, W. H. 2003. Econometric analysis. *Pretence Hall*.

Helton, J. C.; and Davis, F. J. 2003. Latin hypercube sampling and the propagation of uncertainty in analyses of complex systems. *Reliability Engineering & System Safety*, 81(1): 23–69.

Hensman, J.; Fusi, N.; and Lawrence, N. D. 2013. Gaussian processes for big data. *arXiv preprint arXiv:1309.6835*.

Huang, P.; Wang, H.; and Jin, Y. 2021. Offline data-driven evolutionary optimization based on tri-training. *Swarm and evolutionary computation*, 60: 100800.

Jin, Y.; Wang, H.; Chugh, T.; Guo, D.; and Miettinen, K. 2018. Data-driven evolutionary optimization: An overview and case studies. *IEEE Transactions on Evolutionary Computation*, 23(3): 442–458.

Kim, M.; Gu, J.; Yuan, Y.; Yun, T.; Liu, Z.; Bengio, Y.; and Chen, C. 2025. Offline Model-Based Optimization: Comprehensive Review. *arXiv preprint arXiv:2503.17286*.

Kingma, D. P.; and Ba, J. 2014. Adam: A method for stochastic optimization. *arXiv preprint arXiv:1412.6980*.

Koenker, R.; and Hallock, K. F. 2001. Quantile regression. *Journal of economic perspectives*, 15(4): 143–156.

Kursawe, F. 1990. A variant of evolution strategies for vector optimization. In *International conference on parallel problem solving from nature*, 193–197. Springer.

Li, J.-Y.; Zhan, Z.-H.; Wang, H.; and Zhang, J. 2020. Data-driven evolutionary algorithm with perturbation-based ensemble surrogates. *IEEE transactions on cybernetics*, 51(8): 3925–3937.

Li, M.; Li, G.; and Azarm, S. 2008. A Kriging Metamodel Assisted Multi-Objective Genetic Algorithm for Design Optimization. *Journal of Mechanical Design*, 130(031401).

Liu, Z.; Wang, H.; and Jin, Y. 2022. Performance indicator-based adaptive model selection for offline data-driven multiobjective evolutionary optimization. *IEEE transactions on cybernetics*, 53(10): 6263–6276.

Lyu, H.; Herring, D.; Chen, H.; Zhou, S.; Zhang, J.; Wang, L.; Zuo, Z.; Andrews, J.; Spill, F.; Ninic, J.; et al. 2025. A Data-Driven Multi-Objective Optimisation Framework for Energy Efficiency and Thermal Comfort in Flexible Building Spaces. *Energy and Buildings*, 116100.

Lyu, H.; Herring, D.; Wang, L.; Ninic, J.; Andrews, J.; Li, M.; Kočvara, M.; Spill, F.; and Wang, S. 2024. Multi-Objective Optimization for Flexible Building Space Usage. In *2024 IEEE Conference on Artificial Intelligence (CAI)*, 932–939. IEEE.

Mazumdar, A.; Chugh, T.; Hakanen, J.; and Miettinen, K. 2022. Probabilistic selection approaches in decomposition-based evolutionary algorithms for offline data-driven multi-objective optimization. *IEEE Transactions on Evolutionary Computation*, 26(5): 1182–1191.

Paszke, A.; Gross, S.; Massa, F.; Lerer, A.; Bradbury, J.; Chanan, G.; Killeen, T.; Lin, Z.; Gimelshein, N.; Antiga, L.; et al. 2019. Pytorch: An imperative style, high-performance deep learning library. *Advances in neural information processing systems*, 32.

Pedregosa, F.; Varoquaux, G.; Gramfort, A.; Michel, V.; Thirion, B.; Grisel, O.; Blondel, M.; Prettenhofer, P.; Weiss, R.; Dubourg, V.; et al. 2011. Scikit-learn: Machine learning in Python. *the Journal of machine Learning research*, 12: 2825–2830.

Picard, C.; and Schiffmann, J. 2020. Realistic constrained multiobjective optimization benchmark problems from design. *IEEE Transactions on Evolutionary Computation*, 25(2): 234–246.

Romano, Y.; Patterson, E.; and Candes, E. 2019. Conformalized quantile regression. *Advances in neural information processing systems*, 32.

Srinivas, N.; Krause, A.; Kakade, S. M.; and Seeger, M. 2009. Gaussian process optimization in the bandit setting: No regret and experimental design. *arXiv preprint arXiv:0912.3995*.

Steinwart, I.; and Christmann, A. 2011. Estimating conditional quantiles with the help of the pinball loss. *Bernoulli*, 17: 211–225.

Wang, H.; Jin, Y.; Sun, C.; and Doherty, J. 2018. Offline data-driven evolutionary optimization using selective surrogate ensembles. *IEEE Transactions on Evolutionary Computation*, 23(2): 203–216.

Zhang, Z.; Wang, Y.; Liu, J.; Sun, G.; and Tang, K. 2024a. A Two-Phase Kriging-Assisted Evolutionary Algorithm for Expensive Constrained Multiobjective Optimization Problems. *IEEE Transactions on Systems, Man, and Cybernetics: Systems*.

Zhang, Z.; Wang, Y.; Sun, G.; Pang, T.; and Tang, K. 2024b. Constrained probabilistic Pareto dominance for expensive constrained multiobjective optimization problems. *IEEE Transactions on Evolutionary Computation*.

Zitzler, E.; and Thiele, L. 1999. Multiobjective evolutionary algorithms: a comparative case study and the strength Pareto approach. *IEEE transactions on Evolutionary Computation*, 3(4): 257–271.